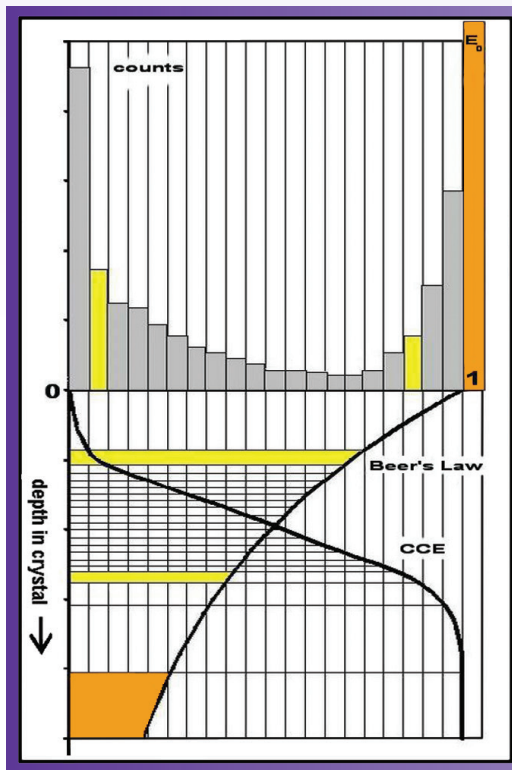


Semiconductor X-Ray Detectors



B. G. Lowe • R. A. Sareen

Semiconductor X-Ray Detectors

Series in Sensors

Series Editors: Barry Jones and Haiying Huang

Other recent books in the series:

Portable Biosensing of Food Toxicants and Environmental Pollutants

Edited by Dimitrios P. Nikolelis, Theodoros Varzakas, Arzum Erdem, and Georgia-Paraskevi Nikoleli

Optochemical Nanosensors

Edited by Andrea Cusano, Francisco J. Arregui, Michele Giordano, and Antonello Cutolo

Electrical Impedance: Principles, Measurement, and Applications

Luca Callegaro

Biosensors and Molecular Technologies for Cancer Diagnostics

Keith E. Herold and Avraham Rasooly

Compound Semiconductor Radiation Detectors

Alan Owens

Metal Oxide Nanostructures as Gas Sensing Devices

G. Eranna

Nanosensors: Physical, Chemical, and Biological

Vinod Kumar Khanna

Handbook of Magnetic Measurements

S. Tumanski

Structural Sensing, Health Monitoring, and Performance Evaluation

D. Huston

Chromatic Monitoring of Complex Conditions

Edited by G. R. Jones, A. G. Deakin, and J. W. Spencer

Principles of Electrical Measurement

S. Tumanski

Novel Sensors and Sensing

Roger G. Jackson

Hall Effect Devices, Second Edition

R. S. Popovic

Sensors and Their Applications XII

Edited by S. J. Prosser and E. Lewis

Sensors and Their Applications XI

Edited by K. T. V. Grattan and S. H. Khan

Semiconductor X-Ray Detectors

B. G. Lowe
R. A. Sareen



CRC Press
Taylor & Francis Group
Boca Raton London New York

CRC Press is an imprint of the
Taylor & Francis Group, an **informa** business

CRC Press
Taylor & Francis Group
6000 Broken Sound Parkway NW, Suite 300
Boca Raton, FL 33487-2742

© 2014 by Taylor & Francis Group, LLC
CRC Press is an imprint of Taylor & Francis Group, an Informa business

No claim to original U.S. Government works
Version Date: 20131017

International Standard Book Number-13: 978-1-4665-5401-6 (eBook - PDF)

This book contains information obtained from authentic and highly regarded sources. Reasonable efforts have been made to publish reliable data and information, but the author and publisher cannot assume responsibility for the validity of all materials or the consequences of their use. The authors and publishers have attempted to trace the copyright holders of all material reproduced in this publication and apologize to copyright holders if permission to publish in this form has not been obtained. If any copyright material has not been acknowledged please write and let us know so we may rectify in any future reprint.

Except as permitted under U.S. Copyright Law, no part of this book may be reprinted, reproduced, transmitted, or utilized in any form by any electronic, mechanical, or other means, now known or hereafter invented, including photocopying, microfilming, and recording, or in any information storage or retrieval system, without written permission from the publishers.

For permission to photocopy or use material electronically from this work, please access www.copyright.com (<http://www.copyright.com/>) or contact the Copyright Clearance Center, Inc. (CCC), 222 Rosewood Drive, Danvers, MA 01923, 978-750-8400. CCC is a not-for-profit organization that provides licenses and registration for a variety of users. For organizations that have been granted a photocopy license by the CCC, a separate system of payment has been arranged.

Trademark Notice: Product or corporate names may be trademarks or registered trademarks, and are used only for identification and explanation without intent to infringe.

Visit the Taylor & Francis Web site at
<http://www.taylorandfrancis.com>

and the CRC Press Web site at
<http://www.crcpress.com>

Contents

Preface	xiii
Acknowledgments.....	xv
Authors.....	xix
Acronyms.....	xxv
Chapter 1: Introduction	1
1.1 <i>Detector and Charge Sensitive Preamplifier: A System Overview</i>	
1.2 <i>Transducers</i>	
1.3 <i>Why Semiconductors?</i>	
1.3.1 <i>Properties of Semiconductors</i>	
1.3.2 <i>Energy Gap</i>	
1.4 <i>Fermi–Dirac Statistics</i>	
1.5 <i>Doping of Semiconductors</i>	
1.5.1 <i>Law of Mass Action</i>	
1.5.2 <i>Depletion Layers and Band Bending</i>	
1.5.3 <i>Schottky Barrier</i>	
1.6 <i>p–n Junction Barrier</i>	
1.6.1 <i>Application of Reverse Bias</i>	
1.7 <i>Charge Generation by Radiation</i>	
1.7.1 <i>Carrier Diffusion</i>	
1.7.2 <i>Signal Development in Electric Field: Shockley–Ramo Theorem</i>	
1.7.3 <i>Recombination</i>	
1.7.4 <i>Trapping and the Hecht Equation</i>	
1.8 <i>Pulse Height Analysis</i>	
1.8.1 <i>Trammell–Walter Equation</i>	
1.9 <i>X-Ray Spectroscopy</i>	
1.9.1 <i>Line Broadening</i>	
1.10 <i>Noise</i>	
1.10.1 <i>Thermal, Johnson, or Voltage Noise</i>	
1.10.2 <i>Dielectric Noise</i>	
1.10.3 <i>Resistive or ‘Contact’ Noise</i>	
1.10.4 <i>Shot or Current Noise</i>	
1.10.5 <i>1/f Noise</i>	
1.10.6 <i>Circuit Noise Analysis and ENC</i>	
1.10.7 <i>Microphony</i>	
1.11 <i>Leakage Current</i>	
1.11.1 <i>Thermal Generation Current</i>	
1.11.2 <i>Diffusion Current</i>	
1.11.3 <i>Surface Leakage Current</i>	

1.11.4	<i>Localise Injection Current</i>
1.11.5	<i>Summary</i>
1.12	<i>Typical Noise Values</i>
1.13	<i>FET</i>
1.13.1	<i>MOSFET</i>
1.13.2	<i>JFET</i>
1.13.3	<i>FET: General Discussion</i>
1.13.4	<i>FET Noise</i>
1.13.5	<i>FET Structures</i>
1.14	<i>Detector Response Function F(E)</i>
1.14.1	<i>Escape Peaks</i>
1.14.2	<i>Low Energy Efficiency</i>
1.14.3	<i>Standards</i>
1.14.4	<i>Summary</i>
1.15	<i>Categorisation of Semiconductor Detectors</i>
1.16	<i>Lithium-Drifted Silicon Detector (Si(Li))</i>
1.16.1	<i>Lithium Drifting</i>
1.16.2	<i>Contouring</i>
1.16.3	<i>Guard Rings</i>
1.16.4	<i>Mechanical Construction: Cryo-Head</i>
1.16.5	<i>Output Waveforms</i>
1.17	<i>Silicon Drift Detectors</i>
1.17.1	<i>Mechanical Construction</i>
1.17.2	<i>Summary</i>
Appendix 1A	
Appendix 1B	
References	

Chapter 2: Detector Response Function 129

2.1	<i>Hypermet Function</i>
2.2	<i>Monte-Carlo Calculations</i>
2.3	<i>Physical Processes and the Analytical Approach</i>
2.4	<i>Peak Broadening—The Fano Factor</i>
2.4.1	<i>Theoretical Calculations of ω and F</i>
2.4.2	<i>Behaviour of ω and F with Energy</i>
2.4.3	<i>Behaviour of ω and F with Temperature</i>
2.5	<i>Charge Collection Efficiency Function</i>
2.6	<i>Generation of Spectral Response Function</i>
2.7	<i>Charge Loss Mechanisms</i>
2.7.1	<i>Escape Peaks</i>
2.7.2	<i>Loss of High-Energy Electrons</i>
2.7.3	<i>Straight Electron Track Model</i>
2.7.4	<i>Simple Charge Diffusion Model</i>
2.7.5	<i>Dead Layers</i>
2.7.6	<i>Very Low Energies</i>
2.7.7	<i>General Radial Dependence</i>
2.7.8	<i>Bulk Trapping</i>

2.8	<i>Charge Gains</i>	
2.8.1	<i>Energetic Electrons from the Contact</i>	
2.8.2	<i>Choice of Metal Contact</i>	
2.8.3	<i>X-Ray Fluorescence</i>	

References

Chapter 3: Detector Artefacts.....173

3.1	<i>Field Distortion</i>	
3.2	<i>Spur</i>	
3.3	<i>Non-Linearity</i>	
3.4	<i>Ghost Peaks</i>	
3.4.1	<i>What Constitutes a Ghost Peak?</i>	
3.4.2	<i>Probable Cause of Ghost Peaks</i>	
3.5	<i>Compton Scattering</i>	
3.6	<i>Self-Counting</i>	
3.7	<i>Absorption Edges</i>	
3.8	<i>Sum Peaks</i>	
3.9	<i>Electron Contamination</i>	

References

Chapter 4: Contacts.....191

4.1	<i>Metal</i>	
4.2	<i>Parameters Influencing ICC</i>	
4.3	<i>Reflection</i>	
4.4	<i>Diffused Junction Contacts</i>	
4.5	<i>Ion-Implanted Contacts</i>	
4.5.1	<i>Double Ion-Implanted Contacts</i>	
4.6	<i>Surface Barrier Contacts</i>	
4.6.1	<i>Amorphous Interface</i>	
4.6.2	<i>Interface States and Recombination</i>	
4.6.3	<i>Dielectric Interface</i>	
4.6.4	<i>Equilibrium and Instabilities</i>	
4.6.5	<i>Methods of Applying a Dielectric</i>	
4.6.6	<i>Quality of Dielectric</i>	
4.7	<i>Low Injection Contacts</i>	
4.7.1	<i>Use of Amorphous Layers in Ohmic Contacts</i>	
4.8	<i>Edge Termination of Contacts</i>	
4.9	<i>Radiation Damage</i>	

References

Chapter 5: Si(Li) X-Ray Detectors.....219

5.1	<i>Manufacture of Si(Li) Detectors</i>	
5.1.1	<i>Selection of Material</i>	
5.1.2	<i>Lithium Diffusion</i>	
5.1.3	<i>Copper Staining</i>	
5.1.4	<i>Machining of Si(Li) Crystal Profile</i>	
5.1.5	<i>Etching</i>	

5.1.6	<i>Lithium Drifting</i>
5.1.7	<i>Initial Drift</i>
5.1.8	<i>Cleanup</i>
5.1.8.1	<i>Electron Trapping for Low-Energy X-Rays</i>
5.1.9	<i>Passivation Theory</i>
5.1.10	<i>Passivation Practice</i>
5.2	<i>Legacy of Contouring</i>
5.3	<i>Losing the Process</i>
<i>References</i>	

Chapter 6: HPSi and HPGe X-Ray Detectors 259

6.1	<i>HPSi X-Ray Detectors</i>
6.2	<i>HPGe X-Ray Detectors</i>
6.2.1	<i>Manufacture of HPGe Detectors</i>
6.2.2	<i>Selection of Material</i>
6.2.3	<i>Lithium Diffusion</i>
6.2.4	<i>Machining of HPGe Crystal Profile</i>
6.2.5	<i>Etching</i>
6.2.6	<i>Passivation</i>
6.2.7	<i>Contacts</i>
6.2.8	<i>Thermal Screening</i>
6.3	<i>Performance</i>
<i>References</i>	

Chapter 7: X-Ray Detectors Based on Silicon Lithography and Planar Technology 271

7.1	<i>Silicon p-i-n Diodes</i>
7.2	<i>Avalanche Photodiodes</i>
7.3	<i>Pixellated X-Ray Detectors</i>
7.3.1	<i>Pileup in PXDs</i>
7.3.2	<i>Charge Sharing</i>
7.3.3	<i>Small Pixel Effect</i>
7.3.4	<i>Hybrid PXDs and ASIC Readout</i>
7.3.5	<i>Performance of Hybrid PXDs</i>
7.3.6	<i>Monolithic PXDs</i>
7.3.7	<i>APS and DEPFET PXDs</i>
<i>References</i>	

Chapter 8: CCD-Based X-Ray Detectors 293

8.1	<i>Introduction</i>
8.2	<i>Techniques of Scientific CCDs</i>
8.2.1	<i>Noise Reduction</i>
8.2.2	<i>Low Energy Sensitivity</i>
8.2.3	<i>High Energy Sensitivity</i>

8.3	<i>Performance of MOS CCD X-Ray Detectors</i>
8.4	<i>pn-CCD</i>
8.4.1	<i>Performance of pn-CCD X-Ray Detectors</i>
8.5	<i>CCDs—Summary</i>
<i>References</i>	

Chapter 9: Silicon Drift X-Ray Detectors.....317

9.1	<i>Introduction</i>
9.1.1	<i>Depletion</i>
9.1.2	<i>Transverse Drift Field</i>
9.2	<i>Concentric Ring SDD X-Ray Detectors</i>
9.2.1	<i>Biasing</i>
9.2.2	<i>Leakage Current in SDDs</i>
9.2.3	<i>Capacitance</i>
9.2.4	<i>Charge Diffusion</i>
9.2.5	<i>Integrated FET</i>
9.2.6	<i>Sensitive Depth</i>
9.3	<i>Droplet SDD X-Ray Detectors</i>
9.4	<i>SDD Performance</i>
9.5	<i>SDD Manufacture</i>
9.5.1	<i>Silicon Wafers</i>
9.5.2	<i>Ring Designs</i>
9.6	<i>SDDs—Summary</i>
<i>References</i>	

Chapter 10: Wide Bandgap Semiconductors349

10.1	<i>Candidates</i>
10.2	<i>General Comments on WBGSs</i>
10.2.1	<i>Ultimate Resolution</i>
10.2.2	<i>Spectral Enhancement Techniques</i>
10.2.3	<i>Polarisation</i>
10.2.4	<i>Crystal Growth</i>
10.2.5	<i>Contacts</i>
10.2.6	<i>Passivation</i>
10.3	<i>Present Status of WBGS X-Ray Detectors</i>
10.3.1	<i>CdTe, CdZnTe, and CdMnTe</i>
10.3.2	<i>GaAs</i>
10.3.3	<i>HgI₂</i>
10.3.4	<i>PbI₂</i>
10.3.5	<i>Diamond and SiC</i>
10.3.6	<i>TlBr</i>
10.4	<i>Summary</i>
<i>References</i>	

Chapter 11: History of Semiconductor X-Ray Detectors and Their Applications.....	381
11.1 <i>Introduction</i>	
11.2 <i>Beginnings</i>	
11.2.1 <i>Search for Materials before World War II</i>	
11.2.2 <i>1930s: Theoretical Understanding</i>	
11.3 <i>Development of Materials during World War II</i>	
11.4 <i>1940–1960: Crystal Counters</i>	
11.5 <i>1940s: Role of National Laboratories, Bell Telephone Laboratories, and Other Corporations</i>	
11.5.1 <i>Field Effect Transistor</i>	
11.5.2 <i>p–n Junction</i>	
11.6 <i>1950s: Radiation Detection</i>	
11.7 <i>1960s: Story of Silicon and Germanium</i>	
11.8 <i>Other Materials</i>	
11.9 <i>1960s: Progress in Detector Manufacture and Spectroscopy</i>	
11.9.1 <i>Centres of Activity</i>	
11.9.2 <i>Semiconductor X-Ray Spectrometers</i>	
11.10 <i>Surface States and Nature's Gift of SiO₂</i>	
11.11 <i>Processing and Passivation</i>	
11.12 <i>1960s: Evolution of Detector Geometries</i>	
11.13 <i>Contacts</i>	
11.13.1 <i>1950s: Diffused Junction Contacts</i>	
11.13.2 <i>1950s: Surface Barrier Contacts</i>	
11.13.3 <i>Engineered Surface Barrier Contacts</i>	
11.13.4 <i>1960s: Ion Implantation</i>	
11.14 <i>1960s: Lithium Compensation</i>	
11.15 <i>1960–1966: Amplifiers</i>	
11.16 <i>1966–1971: Pulsed Optical Restore</i>	
11.17 <i>Applications on the Horizon</i>	
11.17.1 <i>EDXRF Analysis</i>	
11.17.2 <i>Online and Portable EDXRF</i>	
11.17.3 <i>X-Ray Tubes</i>	
11.17.4 <i>Maturity of EDXRF</i>	
11.17.5 <i>EDXMA</i>	
11.17.6 <i>PIXE</i>	
11.18 <i>Companies</i>	
11.18.1 <i>Companies Specialising in WBGSS</i>	
11.18.2 <i>Advanced Photonics, API</i>	
11.19 <i>1970s and 1980s: Evolution in Commercial Environment</i>	
11.19.1 <i>Si(Li) Crystals</i>	
11.19.2 <i>Cryostat</i>	
11.19.3 <i>Cryo-Head</i>	
11.19.4 <i>Case of 'Self-Counting' Detectors and 'Ghost Peaks'</i>	

- 11.20 1970s and 1980s: Low-Energy EDXMA*
 - 11.20.1 'Windowless' EDXMA Detectors*
 - 11.20.2 Question of Nonlinearity*
 - 11.20.3 Icing*
- 11.21 1987: Kevex Quantum Window: Convenience versus Performance*
- 11.22 High-Purity Germanium and Silicon*
- 11.23 1990s: HPGe X-Ray Detectors*
- 11.24 1990s: Bespoke FETs*
- 11.25 Convenience versus Performance: A New Approach*
 - 11.25.1 1990s and 2000s: Enter Lithography and Planar Technology*
 - 11.25.2 Peltier Cooled Detectors (Thermo-Electric Coolers) and Other Cooling Engines*
- 11.26 SDD: Influence of Nuclear Physics Again*
- 11.27 SDDs as X-Ray Detectors*
- 11.28 SDD EDXRS Companies*
- 11.29 Future*
- References*

Preface

The authors waited more than 5 years before recording this detailed account of semiconductor x-ray detectors. During their careers, they witnessed the evolution of the Si(Li) as it gradually replaced early detectors such as scintillators, gas counters, and surface barrier detectors. As will be shown, history has repeated itself and the Si(Li) has now largely been replaced by the silicon drift detector over a period of more than 25 years. It became a welcome relief for many users to relinquish the need to regularly fill their cryostats with liquid nitrogen and to conveniently use detectors using electronic cooling. The one remaining advantage of the Si(Li), its sensitive depth, was not seen sufficiently important compared to the convenience of electronic cooling. Before the knowledge was finally lost, the authors wished to record the science surrounding the Si(Li) and have drawn together this information from industry, government laboratories, and universities. The Si(Li) is restricted to the few special instances where its large sensitive depth is essential. We hope this record will be of interest and an important supplement to the knowledge now required for achieving full understanding of the workings of its replacement, the silicon drift detector.

Acknowledgments

We have both been very fortunate in having the support and patience shown by our families for the many hours we have sat either at a computer or in a library or communicating with former colleagues and associates trying to gather together the information needed for this book.

Many talented people have supported us throughout our careers. In the early days, Rob had a young assistant, Heather Usher, who painstakingly processed the semiconductors and manufactured the early range of detectors needed for Nuclear Physics research at Liverpool and Manchester Universities. Again, while working at Ortec in Oak Ridge, Tennessee, in the early 1970s, Rob appreciated the technical help from the detector R&D group and also the hours spent in lively discussions with Charlie Inskeep, Manny Elad, and John Walter. This pattern of collaboration between physicists and technical specialists became the blueprint for success when transferred into new ventures.

We both enjoyed long careers in industry establishing Link Systems as a leading supplier of detectors, and this pattern was continued later at Gresham Scientific Instruments. During the mid 1980s, we benefitted by acquiring outstanding companies such as Tennelec, The Nucleus, X-tech, and Camscan, and we both enjoyed the collaboration and services of working with talented people from a wide range of disciplines. They were involved not only in the successful development and manufacture of detectors and their associated electronics but also in their promotion into the world markets. This list is understandably long, and we apologise if we have left out any names, but over this period of 40 years there are a number of former colleagues we would like to thank in writing for all their kind efforts and innovations.

In detector manufacturing, we are grateful to Irene Sears and her team for the manufacturing of the Si(Li)s and the HPGe detectors, and in FET manufacturing and assembly we are indebted to Michelle Smith. Claire Whitelock contributed

enormously both in system testing and later in cryostat assembly. Ted Whitehouse led our mechanical design and was a tremendous asset to the business. When Ted retired, Chris Tyrell very successfully continued his work. Our company strategy was always to be the technical leader in our chosen industry and with the help of an enormously talented technical team that included Graham White, Tawfic Nashashibi, Bob Daniel, Chris Cox, Steve Bush, Dave Sareen, and Cos Antoniou, we were at the forefront with innovative products.

Barrie is indebted to the help and assistance given by Stuart Tyrrell while at Link Systems and later Oxford Analytical, and to Irene Sears at Oxford Instruments and Gresham Scientific Instruments, and later to Fang Xiang at Gresham Scientific Instruments. We both benefitted from our work with Greg Bale, Mark Gray, Steve Bush, and all the staff in detector test at Gresham Scientific Instruments.

Acquisitions can often lead to destructive competitive disadvantages and major personality conflicts that ultimately destroy the benefits perceived for the acquisition. Because we were technically led, our acquisitions did not suffer so much from these problems, and we are grateful to Pat Sangsingkeow, Larry Darken, Bruce Coyne, and their colleagues at Tennelec and The Nucleus. It was an enormous pleasure to work with these talented individuals.

Oxford Instruments acquired Link Systems and it was a pleasure to work with Peter Williams, Paul Winson, John Pilcher, and John Woodgate, and it is comforting to see that the former Link Systems microanalysis products are still world leading products.

Gresham Scientific Instruments was established as a division of Gresham Power Electronics, a specialist power supply company and the purchaser of Camscan. Again, this gave both Rob and Barrie the opportunity to work with new people who brought new insights to development and manufacturing. Rob is indebted to the help and wisdom from Mervyn Hobden and the support from Shada Kazami. It was also a pleasure to work with Tony Bosley, Peter Smith, Dave Sareen, Tawfic Nashashibi, Bob Daniel, Greg Bale, Irene Sears, Claire Whitelock, Michelle Smith, and Graham Ensell, and all the other staff who supported this growing business.

Finally, the team efforts from all the other departments in a company are just as vital to its success. We could not have made the advances at Link without our financial team, led by Mac Seaton and then by Danny Weidenbaum. The sales department took on the difficult role of combining end user sales with OEM sales using a direct sales force and agents in many countries. These were ably led by Ron Jones and supported enthusiastically by Roger Bowring, Tom Sheehan, Eric Samuel, Neil McCormick, Frank Brown, Don Grimes, Pat Campos, and many others. The purchasing department under Anne Hart was a constant help to the challenges of a growing business, and the service department under Robin Hart made sure our customers were happy with their installations. Just as a company is no use without a good sales department, it is also extremely difficult to sell a detector without the means of handling the signals generated by the detector. This soon extrapolates into the concept of making a system that can display the histograms and with the appropriate software analyze the complex spectra. For this reason, we have been most fortunate to work alongside expert digital designers such as Brian Sharp, Colin Robinson, and Zaffa Ali, and talented analytical specialists and software designers such as Chris Millward, Peter Statham, Brian Cross, and Will Clark.

To all these people and to many others, we are most appreciative of their contributions to our understanding of the complex physics associated with radiation detection and the challenges in making large numbers of state-of-the art reproducible products that have allowed other scientists to expand their horizons. This probably summarises the difference between studying one device at a university on a research program and having to repeatedly make similar devices in large numbers for a wide range of uses. The challenges are very different, and both are important reservoirs of knowledge. In our own small way, we hope we have documented some of the things we have learned during our time in industry, and we acknowledge that this collection of information is incomplete and biased toward our own experiences and limited understanding of how these devices work.

Authors

School and Universities



B. G. Lowe was born in Chester, UK, and attended Chester City Grammar School and Liverpool University. He graduated with a degree in Physics with distinction in 1962 and with Honours in 1963 and completed his Ph.D. in Nuclear Physics in 1968. He then took a Research Fellowship in Nuclear Physics at Southampton University. His main interest was acoustic spark-chamber particle detectors. He then became a Commonwealth Education Officer based at Colombo University, Sri Lanka, and later took a Lectureship at the Science University in Penang, Malaysia. His research interest was Environmental Radioactivity using low background Ge(Li) detectors. He returned to the UK in 1977 as a lecturer in Physics at the N.E. Wales College of Higher Education.

Industry

Barrie joined Link Systems Ltd UK as chief physicist in 1978, working on the development of lithium-drifted silicon and high purity germanium detectors under Rob Sareen. He became Physics director at Oxford Instruments Microanalysis Group in 1983 as well as head of Development of the Industrial Analysis Group in 1991. The work included the development of a Peltier cooled p–i–n diode and Stirling engine cooled Si(Li) detector for industrial x-ray fluorescence (XRF). From 1993 to 2000, he was senior scientist for the Oxford Instruments

Analytical Systems Division that included the companies X-Tech (x-ray tubes) and Nuclear Measurements Group (large volume HPGe detectors), both based in the United States.

In 1994 he gave the course ‘X-ray Detectors’ at the IEEE Nuclear Science Symposium in Virginia, USA. During the 1990s, he was also involved with the UK Government–sponsored ‘IMPACT’ project investigating novel semiconductor x-ray detectors such as silicon pixel arrays and CCDs. Collaborators included Leicester University, e2v plc, and the Rutherford Appleton Laboratory. He also worked on CdZnTe detectors with Greg Bale (then at Leicester University). From 2000 up to his retirement in 2006, he was senior scientist for e2v Scientific UK, mainly concerned with Si(Li) and HPGe detectors.

Publications and Patents

Barrie was an author on more than 20 publications on radiation detectors and the ‘conditioner’ patent for Si(Li) detectors.

He is married with two sons and two daughters and lives in an Oxfordshire village.

School and Universities



R.A. Sareen was born in Colwyn Bay, North Wales, and attended Colwyn Bay Grammar School. He graduated with a degree in Physics with Honours at Liverpool University in 1963 and then completed a 1-year Graduate Apprenticeship at Rank Bush Murphy in Welwyn Garden City before returning to Liverpool University as a research assistant. Initially, he worked on the design and construction of a Von Ardenne duoplasmatron

and then on Silicon Surface Barrier detectors to measure the ions selected by a magnetic spectrometer attached to this ion

source. The success of this program led to the establishment of a Detector Group to investigate a wide range of detectors to support the researchers at the Accelerators at both Liverpool and Manchester Universities. Detectors included silicon surface barrier detectors for particle physics, lithium-drifted germanium detectors for detecting gamma rays, and lithium-drifted silicon detectors for x-ray measurements. This work led to a Masters Degree in Physics and a consultancy with the pioneering detector company, Ortec Inc., in the United States. Later, Rob returned to Manchester University and completed his Ph.D. in Nuclear Physics.

Industry

In 1968, Rob left with his family to join Ortec as a research scientist in Oak Ridge, Tennessee. He worked in the company's Detector Group, designing both linear and radial position-sensitive particle detectors with some of the pioneers on silicon and germanium detectors including John Walter, Rex Trammell, Emmanuel Elad, and Charlie Inskeep. Rob also investigated new front contacts for silicon particle and x-ray sensors.

After a period of 4 years, he returned to the UK to establish a detector company initially called Nuclan Ltd. Factors instrumental to making this decision included the offer of a government grant from the Department of Industry and the knowledge of the exciting work on time variant pulse processing by Wrangy Kandiah's Group at UKAEA Harwell. Also, Kevex, a California-based company, had just released an optical restoring x-ray spectrometer and Ortec had decided it did not want to pursue this technology, but instead focus its efforts on the growing opportunities in germanium gamma ray detectors.

Nuclan quickly merged with Link Systems Ltd., a recently formed analytical company making a computer-controlled energy dispersive analyzer to work with imported Kevex x-ray detectors. Rob, in his role as technical director, introduced a range of silicon x-ray spectrometers based on the principles of

lithium drifting to form deep structures for absorbing x-rays up to 30 keV. The company grew rapidly during the 1970s with successes in Europe, the USSR, and the United States.

In 1980 the company was acquired by a leading UK plc, UEI, and Rob became managing director of the Link Scientific Group and a main board director of UEI. The Link Group grew rapidly during this period and also acquired X-Tech in California, a company specialising in X-ray Tubes, and then The Nucleus in Tennessee, the owners of Tennelec, a nucleonics company.

Carlton Communications purchased UEI in the late 80s and then sold the Link Scientific Group to Oxford Instruments. Rob joined the Oxford Group as an executive director responsible for the Link Group of Companies and the XRF Analytical business that Oxford had grown.

In 1992, Rob left industry and returned to academia at Manchester University for 2 years and then returned into industry having purchased Gresham Power Electronics in Salisbury and Camscan in Cambridge. Gresham introduced a range of sensors to satisfy the needs of a growing number of specialist analytical companies that had the computer and software skills but needed an appropriate sensor to make an analytical instrument. Gresham was acquired by e2v in 2006 and is now firmly established as a successful supplier of a wide range of x-ray sensors.

Awards and Publications

Rob was awarded an MBE in 1991 for Services to Science and became a Fellow of the Institute of Physics in 1986. He is also a Fellow of the Royal Microscopical Society.

Link Systems was awarded Queens Awards for both Technology and Export and an R&D 100 award from the United States. In 1999, he was awarded the Presidential Science Award for 'Outstanding Contribution to the Theory and Practice of Microbeam Analysis' by the Microbeam Analysis Society.

During his working career, he liaised with several government departments including the Security Services and met with the Prime Minister, Margaret Thatcher, several times to discuss the challenges of growing UK businesses in an international market. He has also participated as a committee member on topics such as Nuclear Strategy and Home Land Security. He is married and has two sons living in Marlow, Buckinghamshire.

Rob authored more than 15 publications on radiation detectors and holds two patents.

Acronyms

a-C	Amorphous Carbon
AEC	Atomic Energy Commission (USA or Australia)
AEI	Associated Electrical Industries
AEM	Analytical EM
AERE	Atomic Energy Research Establishment, UK
a-Ge	Amorphous germanium
ANU	Australian National University
APD	Avalanche photodiode
APS	American Physical Society
a-Si	Amorphous silicon
ASIC	Application-specific IC
ASM	Associated Semiconductor Manufacturers Ltd., UK
ASTM	American Society for Testing and Materials
AT&T	American Telephone and Telegraph (became Bell Telephone Co.)
ATW	Atmospheric pressure–supporting thin window
AWRE	Atomic Weapons Research Establishment, UK
BNL	Brookhaven National Laboratory, USA
BTH	British Thomson-Houston Co.
CCD	Charge coupled device
CCE	Charge collection efficiency
CDS	Correlated double sampling
CEA	Nuclear Energy Research Centre, Saclay, France
CEN	Nuclear Energy Research Centre, Saclay, France
CEO	Chief executive officer
CERN	European Organisation for Nuclear Research, Geneva
CES	French Atomic Energy
CFTH	French Thomson-Houston Co.
CMOS	Complementary MOS
CNRS	Centre National de la Recherche Scientifique, France

CP4	Silicon or germanium etchant
CPPM	Centre de Physique des Particles de Marseille, France
CRO	Cathode ray oscilloscope
CSF	Compagnie Generale de Telegraphie sans Fils, France
CTE	Charge transfer efficiency (CCDs)
C-V	Capacitance–voltage (plot)
CVD	Chemical vapour deposition
DEPFET	Depletion-mode FET
DI	Deionise (high resistivity) water
DoE/D	Department of Energy/Defence (USA)
e2v	Originally English Electric Valve (EEV) Co., UK
EDX	Energy dispersive x-ray spectrometry
EDXMA	Energy dispersive x-ray microanalysis
EDXRF	Energy dispersive x-ray fluorescence
EDXRS	Energy dispersive x-ray spectrometry
EG&G	Edgerton, Germeshausen and Grier Co., USA
EM	Electron microscope
EMP	Electron microprobe
EMRS	European Materials Research Society
ENC (enc)	Equivalent noise charge
EPA	Electron probe analysis
epi-Si	Epitaxial grown Si
EPMA	Electron probe microanalysis
ESA	European Space Agency
ESCA	Electron spectroscopy for chemical analysis
ESTEC	European Space Research and Technology Centre, Netherlands
ETH	Eidgenössische Technische Hochschule, Zürich, Switzerland
EXAFS	Extended x-ray absorption edge fine structure
FBC	Feedback capacitor
FET	Field effect transistor
FWHM	Full-width half-maximum
FZ	Float zone
GE	General Electric, USA

GEC	General Electric Company, UK
Ge(Li)	Lithium-drifted germanium
GKSS	Helmholtz Research Centre, Germany
G-R	Guard ring
HEP	High energy physics
HNU	Manufacturer of Photo-Ionisation Detectors, USA
HPB	High-pressure Bridgman (crystal growth)
HPGe	High-purity Ge
HPSi	High-purity Si
HTO	High take-off (angle)
HV	High voltage
IAEA	International atomic energy authority
IC	Integrated circuit
ICC	Incomplete charge collection
IEEE	Institute of Electrical and Electronics Engineers
IMO	Inverted mode operation (same as MPP)
INR	Institute of Nuclear Research, Poland
IOP	Institute of Physics, UK
IR	Infrared
IRE	Institute of Radio Engineers (became IEEE)
JEOL	Japanese Electron-Optics Labs Ltd.
JFET	Junction FET
JPL	Jet Propulsion Laboratory, USA
KAPL	Knolls Atomic Power Laboratory, USA
KEK	Japanese synchrotron center
LALC	Large area, low capacitance
LBL	Lawrence-Berkeley National Laboratory, USA
LEC	Liquid encapsulated Czochralski (crystal growth)
LED	Light-emitting diode
LHC	Large Hadron Collider, CERN
LLNL	Lawrence Livermore National Laboratory, USA
LN	Liquid nitrogen
LPB	Low pressure Bridgman (crystal growth)
LT	Compagnie Lignes Telegraphiques et Telephoniques, France

MAS	Microbeam Analysis Society
MBE	Molecular beam epitaxy
MCA	Multichannel analyzer
MDL	Minimum detectable limit
MIT	Massachusetts Institute of Technology, USA
MOS	Metal oxide semiconductor (technology)
MOSFET	Metal oxide semiconductor FET
MPI	Max Planck Institute, Germany
MPP	Multipinned phase (same as IMO)
MRS	Materials Science Society, USA
MUX	Multiplexing
NAA	Neutron activation analysis
NAS	National Academy of Sciences, USA
NASA	National Aeronautical and Space Administration, USA
NBS	National Bureau of Standards, USA
NE	Nuclear Enterprises Ltd., UK
NEC	Nuclear Equipment Corporation, USA
NIM	Nuclear Instrumentation Module
NIM	<i>Nuclear Instruments & Methods in Physics Research</i> (journal)
NRC	National Research Council, USA
NRD	Nuclear Radiation Development, Canada
NRDL	Naval Radiological Defence Laboratory, USA
N-S	IEEE Nuclear Science Symposium
NSI	Nuclear Semiconductor Inc., USA
NTD	Nuclear Transmutation Doping
NYO	New York Operation Office (USAEC)
OI	Oxford Instruments plc. UK
ORNL	Oak Ridge National Laboratory, USA
PAD	Pixel array detectors
P/B	Peak-to-background ratio
PCB	Printed Circuit Board
PGT	Princeton Gamma Technology Inc., USA
PHA	Pulse height analysis (or analyzer)
p-i-n	p-intrinsic-n type silicon diode structure

PIXE	Particle-induced x-ray emission
pn-CCD	p-n junction CCD
poly-Si	Polycrystalline Si
PSD	Position-sensitive detector
PSG	Phosphosilicate glass
PTFE	Teflon
PTIS	Photothermal ionisation spectroscopy
PVC	Polyvinyl chloride
PXD	Pixel (x-ray) detectors
QE	Quantum efficiency
R	Rads (Roentgen x-ray dose)
RAL	Rutherford-Appleton Laboratory, UK
RC	Resistance Capacitance product (time constant)
RCA	Radio Corporation of America, USA
RF	Radio frequency
RIDL	Radiation Instrument Development Laboratory, USA
RMD	Radiation Monitoring Devices, USA
rms	Root mean square deviation
RT	Room temperature
RTC	La Radiotechnique, France
RW	Ramo-Wooldridge Co., USA
SBIR	Small business innovative research
SCD	Swept charge device
SDD	Silicon drift detector
SEM	Scanning EM
SERL	Services Electronics Research Laboratory, UK
Si(Li)	Lithium-drifted silicon
SOG	Spin-on glass
SPIE	Society of Photographic Instrumentation Engineers, USA
SSR	Solid State Radiations Inc., USA
T	Absolute temperature in Kelvin
TCE	Trichloroethylene
TEC	Thermo-Electric (Peltier) cooler
TEM	Transmission EM
THM	Travelling heater method (crystal purification)

TI	Texas Instruments Inc., USA
TMC	Technical Measurements Corporation, USA
TUM	Technical University Munich, Garching, Germany
TW	Thin (x-ray) window
TXRF	Total reflection XRF
UCRL	University of California Lawrence Radiation Laboratory (report)
UEI	United Engineering Industries, UK
UHV	Ultrahigh vacuum
UKAEA	United Kingdom Atomic Energy Authority
URS	United Research Services, USA
USAEC	United States Atomic Energy Commision
UTW	Ultrathin (x-ray) window
VG	Vacuum Generators Ltd., UK
VLSI	Very large silicon IC
VP	Vice president
WBGS	Wide bandgap semiconductors
WDS	Wavelength dispersive spectrometry
WDXRF	Wavelength dispersive XRF
WW2	World War 2
XAFS	X-ray absorption edge fine structure
XMM	X-ray multi mirror satellite
XRF	X-ray fluorescence
XRS	X-ray spectrometry (also a journal)

1

Introduction

Since 1950, we have witnessed the development of a range of radiation detectors exploiting the properties of semiconductor materials. The progress has been documented in many textbooks, some of which are listed in chronological order in Appendix 1A. We have also added a list of books that cover certain aspects of semiconductor x-ray detectors where the main topic is x-ray analysis.

It may legitimately be asked, ‘Why do we need another book on the subject?’ To answer that, we note that there has been rapid progress recently in devices such as silicon drift detectors (SDDs) and charge-coupled devices (CCDs) and renewed interest in alternative materials such as CdZnTe and diamond. This makes the choice of detector for particular applications rather bewildering for potential users and it has become necessary to compare their characteristics with the lithium-drifted silicon ‘Si(Li)’ x-ray detectors that have been the mainstay of the x-ray scientists using semiconductor detectors. Added to this, the practical construction and historical development of these detectors has not, to date, been given its just exposure in detail. The high-purity germanium (HPGe) detector has been shown to have superior qualities to the Si(Li) detector in many of its characteristics and the reasons for its present lack of application and availability need to be aired.

Going back even before the dawn of semiconductor detectors, Serge Korff [1] wrote in 1946 in the preface to his book, *Electron and Nuclear Counters* (published by Van Nostrand),

It is the purpose of this book to gather together and summarise the facts regarding the theory of the discharge mechanism and the

practical operation of various types of counters. Although they have been known for about forty years, they are even today surrounded by an atmosphere of mystery and their construction and operation are claimed by many competent scientists to involve ‘magic’. Various laboratories have developed special procedures for their manufacture and use, often without knowing why particular techniques appear to be successful.

That book concerned *gas proportional detectors*, but Korff’s remarks could apply equally well today when looking back over the 40-odd years since the ‘maturity’ of the Si(Li) x-ray detector in the mid to late 1960s. Gas detectors are still manufactured and the technology is still difficult, as is that for semiconductor x-ray detectors. Indeed, even as early as 1970, Fred Goulding [2] of the Lawrence Radiation Laboratory wrote:

Work on ultra-high resolution spectrometer systems using semiconductor detectors has been excessively time-consuming, and, for the most part frustrating. To my knowledge this remark has been true (if we include ionisation chambers) for the past 25 years although the details have changed.

It is interesting to note that CdZnTe and SDD detectors are now reaching their ‘maturity’ in terms of applications, but the gestation time again has been in the order of 20 and 30 years, respectively. Even in the case of Si(Li) detectors, some areas are still not well understood after nearly 50 years of ‘maturity’. It is our hope that this book will explain the painful evolution of semiconductor x-ray detectors and will remove at least some of the ‘magic’ involved in their construction.

It should be explained at the outset that this book is not a textbook on semiconductor physics or electronics and will give only as much of the theory as is required to describe the principles of the detectors. If further theoretical details are required, references are made to where this can be found. Instead, this book will concentrate on the principles of the semiconductor transducers themselves. Some attention will be given to the field effect transistor (FET) that developed historically with the transducer and shared many of its manufacturing problems (material, surface states, noise) and ended, in practice, closely coupled (indeed sometimes integrated) with it.

Because both are usually cooled, this union is often referred as a ‘cryo-head’.

Semiconductor detectors were first used in nuclear physics research as particle detectors for electrons, protons, alpha particles, and—with a suitable converter—neutrons. They were also almost immediately used to try to measure gamma rays and x-rays. Information on the developments of associated materials and measuring electronics is abundant in the scientific literature. In this book, we attempt to bring some of this information together and, where possible, credit the innovators. Our focus will be on how these developments paved the way for the modern x-ray sensor.

Our perspective as participants in the industries created by these detector developments enables us to bring a working view of how both the science and the companies involved progressed. We will focus on x-ray detectors made from silicon in the main as used in the x-ray microanalysis and XRF (x-ray fluorescence) industry, but we will also cover the use of germanium and other semiconductors.

Our searches through the scientific journals and the various technical books has shown how history often repeats and also how recognition of creative thought can be confused and misinterpreted. Both government scientists and industrial scientists are sometimes limited in what they can publish, and many universities and institutions have allegiances with industry that can produce similar restrictions. These constraints tend to dissolve with time, and we have been fortunate enough to examine many technical journals; some of these are now available on the Internet. Some information, as for example on the development of FETs, was held in the National Archives in the UK and was subjected to restrictions that have now been released under the 30-year rule. Other information has been assembled from both company published articles and by conversations with some of the people involved in the history of the development, the manufacturing, and the marketing of these devices. Putting this all together has taught us how important it is for young engineers and scientists to examine the early work and to make use of the excellent online search techniques available for reviewing literature and patents. In particular, and where appropriate,

we reproduce text and drawings from the patents and papers to give a meaningful time-base to these developments. Many hours spent on reading these patents have demonstrated what a fertile source of information they are regarding both the science and the claimed invention.

Our working knowledge of the x-ray spectroscopy industry while these developments were progressing has been supplemented with information from conversations with other similarly placed scientists and engineers. Our researches have shown how the development of semiconductor radiation detectors tracked the development of semiconductor materials and semiconductor devices such as diodes, transistors and integrated circuits (ICs). The technical challenges that had to be overcome to produce the detectors in current use depended on the parallel development of FETs, as noted earlier, as well as on x-ray transmission windows and signal processing electronics. In the following, we use 'FET' to define the family that includes junction field effect transistors (JFETs) and metal oxide semiconductor FETs (MOSFETs). Most of the x-ray detectors needed cryostats constructed from the correct materials with efficient thermal design and freedom from vibration effects. It is our intention to review the development of all the key components that were required for today's x-ray spectrometers and to show how the various sensors evolved. The overview that follows will describe the essentials without entering the details that will, in many cases, be discussed in later chapters. It is hoped that this Introduction and the details that will be discussed next (Chapters 2 through 10) will help to set the history (Chapter 11) in perspective. Chapter 11 can be omitted, but it does shed light on why the detectors evolved, rightly or wrongly, in the way they did.

1.1 Detector and Charge Sensitive Preamplifier: A System Overview

To give an overview, it is instructive to consider the electronic circuit representing the basis of most semiconductor x-ray detectors (Figure 1.1).

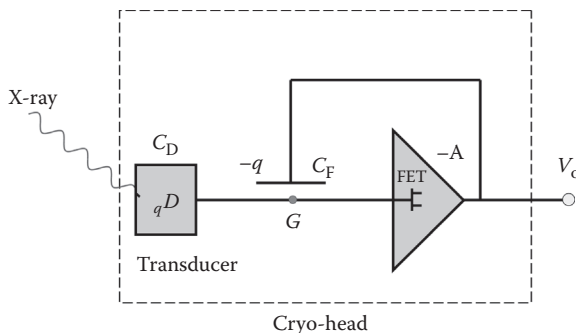


Figure 1.1 X-ray sensor front end or cryo-head.

Here, ‘ $-A$ ’ represents the preamplifier open loop-gain that, by negative feedback through the capacitor C_F , maintains point G at a virtual ground potential. The first stage of the preamplifier is the FET. If a charge q has accumulated at G (by ionisation due to an x-ray passing into the transducer D or by leakage currents into G), then the virtual ground is maintained by the preamplifier reacting to pump an equal and opposite charge $-q$ onto C_F . This results in an output voltage

$$V_o = -q/CF. \quad (1.1)$$

This is a simple negative feedback circuit by way of the capacitor, the feedback capacitor (FBC), C_F , to one electrode of the transducer D and the gate of the FET. Its simplicity, however, belies the physical and engineering difficulties in realising such an arrangement capable of resolving x-rays of energies of the order of 100 eV (or about 30 electrons in silicon) up to more than 20 keV. The FET gate G represents a very high impedance point in the circuit, and any charge that accumulates there has virtually no leakage to true ground. In the absence of some charge reset mechanism, the FET would be driven off its linear excursion and introduce signal distortion. The practical methods of providing such a mechanism proved to be just one of the technological challenges.

Considering the absorption of x-rays in matter, we expect the fraction of intensity absorbed $-dI/I$ to be proportional to the incremental penetration depth, dx

$$\frac{dI}{I} = -\frac{dx}{L},$$

where L is a constant for any given material and x-ray energy and has dimensions of length. The result of integrating this is an equation known as Beer's law,

$$I = I_0 \exp(-x/L),$$

where I_0 is the x-ray intensity at surface $x = 0$, and L is the reciprocal of the 'linear absorption coefficient' of the absorbing medium. As the absorption in matter is a strong function of its density ρ , it is most often written as

$$I = I_0 \exp(-\mu_a \rho x), \quad (1.2)$$

where μ_a is the mass absorption coefficient and generally decreases with increasing x-ray energy. It will be noticed that the most probable depth for absorption in a uniform medium is always near $x = 0$ (i.e., at the surface). As an example, Figure 1.2 shows the attenuation of 20 keV x-rays in silicon and 50 keV x-rays in germanium using the published values of μ_a .

It is seen that approximately 3 mm depth of silicon or equivalent is required for reasonable efficiency at 20 keV. Germanium at this depth is efficient up to ~100 keV. Incidentally, GaAs being a compound of elements either side of germanium in atomic number, has a similar attenuation to it. As a result of the quantisation of the electron energy levels in atoms, the mass absorption coefficients have step discontinuities, known as absorption edges. For example, as the x-ray energy moves from below to above the binding energy of the K-shell (see Section 1.3.2) electron (1.84 keV in silicon and 11.1 keV in germanium), there becomes enough energy to release the electron and the absorption coefficient steps up in magnitude at these energies. These discontinuities are not shown in Figure 1.2.

The detector is based on the principle that the charge generated by the absorption of the x-ray in the transducer is proportional to the energy of the x-ray. It is important to realise that the exponential decay in intensity of low-energy

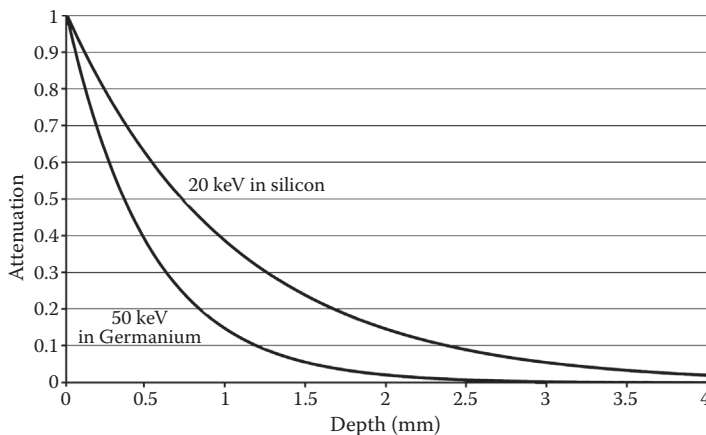


Figure 1.2 Attenuation of x-rays in silicon and germanium.

x-rays described by Beer's law above (with the absorption edge discontinuities) does not in any way affect the *energy* of the x-rays. This is unlike charged particles that lose energy quasi-continuously along their path. Thus, from a spectroscopic viewpoint, it is more important that the charge generated is fully accounted for than that x-rays are not absorbed in any 'dead layers' (including any x-ray window). In other words, that all such charge is contained in the active volume of the transducer and there are negligible contributions from absorption from outside it.

To achieve the low x-ray energy threshold sensitivity, the noise must be reduced and the transducer and the FET must be cooled, but not necessarily to the same temperature. For sensitivity using silicon, the transducer must be 3 mm or more in diameter and so the active volume is $\sim 30 \text{ mm}^3$ or more. This is in complete contrast to the microelectronic development that has taken place in silicon technology driving the dimensions smaller and smaller. The cryo-head must be screened from extraneous electrical, magnetic, radiation, and vibrational interference, and the virtual ground (G in Figure 1.1) must present the lowest possible capacitance as it is connected to the gate of the FET and the FET noise depends on its capacitive loading. This capacitive loading includes the transducer capacitance, C_D , the gate capacitance

of the FET, C_F , and any stray capacitance, C_S . In practice, this means that the physical size of the conductor at G (the transducer electrode and FET gate contact) must be restricted, and there must be virtually no changes in C_F and C_S (both of the order of a fraction of a pF) due to vibration (microphony). Another source of noise is the dielectric used to hold these components together, and care must be taken in selecting materials. Added to these impositions, in electron microscope (EM) applications, the cryo-head needs to be on the end of a long probe (typically 30–50 cm) and typically 12–16 mm in diameter. We will discuss how such transducers and FETs can be manufactured, and how the other conditions can satisfactorily be engineered.

1.2 Transducers

The transducer converts the energy E of the x-ray entering it into an electrical signal, usually in the form of charge q induced onto the electrode connected to G in Figure 1.1. The major part of this book will be devoted to the transducer, its physical properties, manufacture, and evolution. If we are to measure E in terms of q , it is clear that q should represent *all* of energy E , which should in turn be completely absorbed in the transducer. It would also be advantageous if they were directly proportional. Or, in terms of the number n of *electronic* charges e , for example

$$q = ne$$

$$E = \omega n, \quad (1.3)$$

where ω is a constant. This constant ω (measured in eV) represents the x-ray energy required to induce one electronic charge onto G and is a characteristic of the absorbing medium.

We can picture the process using the gravitational analogy of dropping a coin into a glass of beer (say), as depicted in Figure 1.3.

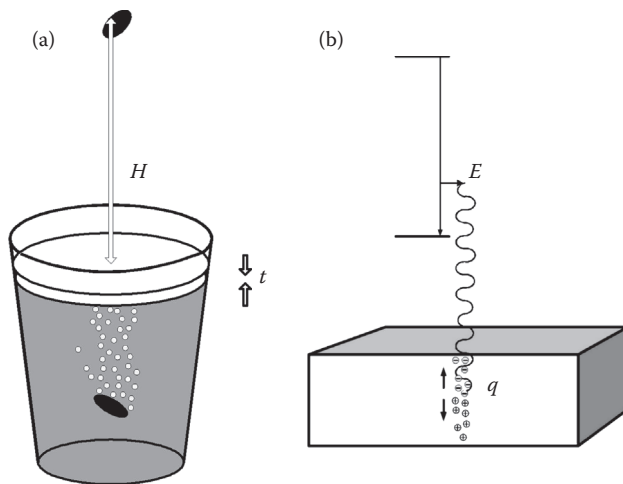


Figure 1.3 Coin dropped into a liquid. (a) Pebble in a liquid and (b) x-ray absorbed in matter.

X-ray detectors rely on the linearity between energy absorbed and charge collected. The number of bubbles liberated (say, thickness t of froth) is proportional to the potential energy (height) of the coin. The x-ray emitted from the atomic level transition is fully absorbed in the solid and by ionisation, generates charge q on the electrode.

The absorption of x-rays is stronger, in general, in solids than in liquids or gases. The specific absorption (mass absorption coefficients, μ_a) and density of the solid has to be a consideration for the more penetrating higher energy x-rays (or gamma rays) because spectroscopy relies on the total absorption of the incoming x-ray energy. At the energies under consideration, photoelectric absorption (where the x-ray energy is transferred to an atomic electron producing a ‘photoelectron’) is dominant, but scattering (Compton scattering) of the x-ray may be significant in the higher energy range. Compton scattering of an x-ray is the ‘billiard ball’-like collision of the photon by an atomic electron. The probability of scattering is proportional to the number of electrons available (atomic number Z) and is very low in silicon at the energies we are mainly concerned with (below 20 keV). In photoelectric absorption, the atom of the absorbing medium

is left in an excited state and can relax by the emission of a fluorescence x-ray, but this is usually also absorbed back into the medium. The probability of photoelectric absorption varies as a high power (~ 4.5) of the atomic number Z of the atom involved, which explains the higher absorption in germanium relative to silicon of the same energy x-ray (Figure 1.2). Higher Z materials have advantages of high efficiency in the case of higher energy (more penetrating x-rays and gamma rays). The reduced energy of the Compton scattered x-ray and the energy of the recoil electron are also usually absorbed. Charged particles, such as electrons, have shorter ranges and are all usually stopped in thick detectors.

The energy of the photoelectron is equal to the energy of the absorbed x-ray minus the atomic binding energy of the absorbing electron. The emission of the photoelectron leaves behind a hole. This 'hole' is filled by an electron from a higher atomic level, followed by the emission of a fluorescence x-ray or an Auger ('O-J') electron (Figure 1.4). The photoelectron (and Auger electron, if emitted) is usually reabsorbed back into the transducer. It should be pointed out that with Compton scattering through wide angles and subsequent photoelectric absorption, even a thin detector totally absorbs some high-energy events. The higher density solids are preferred for the higher energy range of x-ray spectrometry to

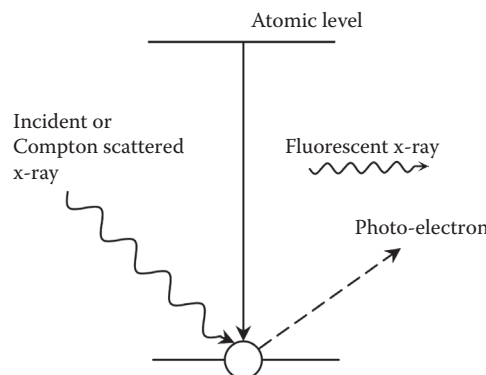


Figure 1.4 Radiation loss processes.

improve the detectors efficiency, and in this respect solid-state detectors are preferred to gas proportional detectors in most cases. If we are to measure the free charge generated in a solid volume, it is clearly advantageous also if the volume does not already contain free charge. Using our gravitational ‘glass of beer’ detector analogy, it would not be very effective if the beer were full of bubbles to begin with (cool beer is best!). This immediately rules out metals. In fact, it is the free charge at the surface of metals that gives the metal surface its reflective lustre. Insulators normally have a dull surface and semiconductors (such as graphite, silicon, and germanium) only a partial lustre. It would seem from this point of view that insulators or ‘semi-insulators’ should be best and, in fact, these were the first to be used (crystal detectors) and are still used (materials such as mercuric iodide, diamond) when cooling is not possible, convenient, or necessary.

The fast-moving photoelectrons and Auger electrons ionise the solid in a cascade of charge generation, and the transducer can be regarded as a ‘charge amplifier’. Looking at Equation 1.3, it is seen that the inverse of ω is a measure of the sensitivity or ‘intrinsic charge gain’ of the transducer. The smaller ω becomes, the greater is the charge signal q for a given value of E . With modern FET amplifiers, this is not a significant issue (substituting $C_F = 0.01 \text{ pF}$ into Equation 1.1 gives $V_o \sim 6 \mu\text{V}$ even for just a million electrons). However, the *statistical spread* of the signal is important. This is given by the statistical spread in the number n , and in Poisson statistics this would be \sqrt{n} . So, the relative width (or ‘resolution’) of the distribution in n might be expected to be $\sqrt{n}/n = 1/\sqrt{n}$. We will see later that because all of the energy E is not converted to charge, even for complete absorption, the spread in n is actually given by \sqrt{Fn} rather than \sqrt{n} . Here, F is the celebrated Fano factor that, apart from ω , is the next most important parameter for the absorbing medium. It is quite surprising, however, that the value of F (first calculated for gases by Ugo Fano [3] in 1946 and is ~ 0.1) does not vary much from one absorbing medium to another, even from solids to gases.

1.3 Why Semiconductors?

Semiconductors have higher intrinsic gains because bound electrons are more easily broken free, for example, by radiation or heat, and have ω measured in just a few eVs. The rare gases have values of a few 10s of eV. The ‘Cooper pairs’ of bound electrons found at very low temperatures (liquid helium ~2 K) in superconductors have binding energies of the order of a few meV and give much higher sensitivity and resolution detectors. Apart from the very low temperature superconducting and bolometer detectors, which have their own cost and technology problems and are not the topic of this book, semiconductors therefore appear to be the most attractive.

The values of ω (or ionisation energy) for a number of gases, semiconductors, semi-insulators, and insulators are given in Table 1.1 (see also Table 10.1).

TABLE 1.1
Value of ω (or Ionisation Energy) for Specified Materials

Medium	Formula	Atomic Number Z (Average)	Density (gm/cm ³)	Average Energy per Electron–Hole Pair (eV)
Neon gas	Ne	10	0.9×10^{-3}	36.2
Argon gas	Ar	18	1.7×10^{-3}	26.2
Xenon gas	Xe	54	5.9×10^{-3}	21.5
Silicon dioxide (quartz)	SiO ₂	15.3	2.2	17
Silicon	Si	14	2.3	3.65
Germanium	Ge	32	5.3	2.96
Gallium arsenide	GaAs	31.3	5.4	4.3
Mercuric iodide	HgI ₂	80.53	6.4	4.2
Lead iodide	PbI ₂	82.5	6.2	7.68
Cadmium telluride	CdTe	48.5	6.1	4.4
Silicon carbide	SiC	10	3.12	7.8
Diamond	C	6	3.5	13.25

There is, however, the problem of free quiescent charge in the semiconductor bulk. Even if the temperature is lowered to liquid nitrogen temperature (LNT) (77 K), as was done with the early crystal detectors, there is sufficient free bulk charge to add to the statistical broadening (noise). It took some time for users to realise that semiconductors had another unique advantage, however. They can be fabricated in such a way as to *deplete* the bulk of its free charge, thereby revealing a highly x-ray–sensitive layer. This was achieved by forming a reverse bias p–n junction *diode*. To explain this, we need to look at the properties of semiconductors that make them so special.

1.3.1 Properties of Semiconductors

From the earliest investigations of electrical conduction, solids fell into the well-separated categories of insulators and conductors. This turned out to be extremely convenient practically for the development of electricity as the free charge conduction in one conductor (e.g., copper) could be isolated (e.g., by ceramic or a plastic coating) from that in another. Then, in the late 1800s, it became clear that there was a category of solids, ‘semiconductors’, which fell between the two. In fact, unlike metals, their conductivity increased with temperature and illumination. Then in the 1970s, it was discovered that even some plastics (conjugated polymers) could conduct electricity. The range is illustrated in Figure 1.5.

1.3.2 Energy Gap

The explanation for these differences lies in the ‘electronic band structure’ of the materials. Electrons can only occupy specific energy levels and in solids these levels form bands, each of which can only accommodate a certain number of electrons because of the quantum mechanical exclusion principle for electrons. This stipulates that only one pair of electrons (one spin up and one spin down) can occupy any energy level in a quantum mechanical system such as an atom. In metals, the highest band is only partially occupied and is known as the conduction band. In it, the electrons are free to

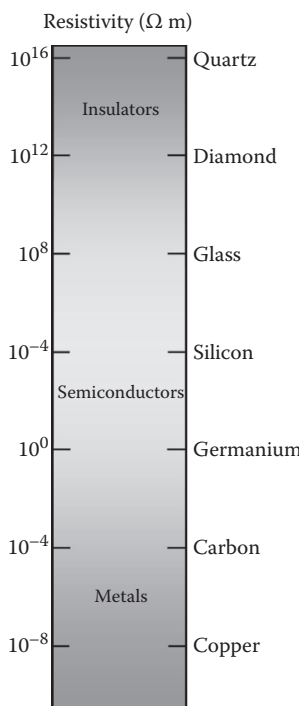


Figure 1.5 Resistivities of various materials.

move under the influence of an applied electric or magnetic field. In insulators, the conduction band is empty and the highest occupied band is the valence band. The valence band is occupied by electrons that are bound and localised (to a greater or lesser extent) to the atom. All states are occupied and because of the exclusion principle, no electron is free to move as the surrounding states are already occupied. The energy gap (E_g) between them is so great ($E_g > 10 \text{ eV}$) that electrons are energetically incapable of leaping this gap at normal temperatures and electric fields, and no conduction takes place.

The same situation also exists in semiconductors, but here the energy gap E_g is less (a few eV) and electrons can, under several circumstances, leap from the valence band into the conduction band. This is illustrated schematically in Figure 1.6.

In metals, the highest occupied bands are only partly filled, and they can conduct electric charge. In insulators, the

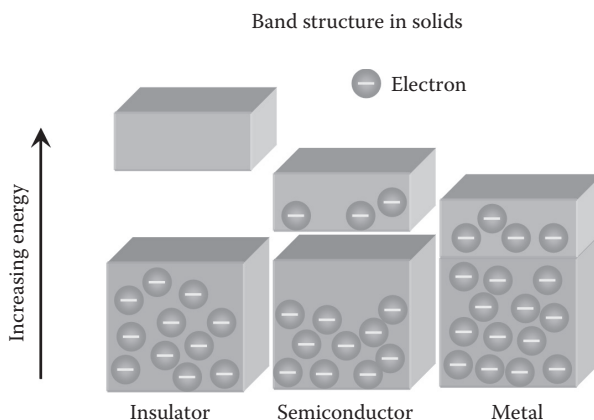


Figure 1.6 Electrons available for conduction in materials with a small, medium, or no bandgap.

highest occupied bands are filled and are separated from the next empty band by an energy gap. If the energy gap is small enough, electrons stimulated by heat or radiation can jump from the valence band to the conduction band and the material is a semiconductor. To see how the energy gap arises, we turn to the structure of atoms and the periodic table of elements. As we increase the number of atomic electrons (atomic number Z) because of the exclusion principle, they fill the available levels in sequence. The first few levels and their maximum occupancy are 1s(2), 2s(2), 2p(6), 3s(2), and 3p(8), and because of the way their energies are distributed they form closed ‘shells’—1s(2), 2s–2p(8), and 3s–3p(8). These are given notations (K, L, M, etc.). This gives the periodic table and the grouping of elements with similar chemical and physical properties as shown below.

The center of the table (Group 4 elements, highlighted red in Figure 1.7) represents atoms with an outer shell of four electrons and hence four empty levels in the outer valence shell. The shell of any such atom can be ‘quasi-completed’ by bringing four other atoms into close proximity so that electrons can be ‘shared’. This sharing forms four ‘covalent bonds’. This is shown schematically in two dimensions in Figure 1.8 for the case of silicon.

Group	1	2	3	4	5	6	7	0
	1							2
	H							He
3		4	5	B	6	C	7	N
	Li	Be		B		C		N
11		12	13	Al	14	Si	15	P
	Na	Mg		Al		Si		P
19		20	31	Ge	32	As	33	Se
	K	Ca	Ga	Ge		As		Se
								Br
								Kr

Transition elements

Figure 1.7 (See colour insert.) Part of the periodic table.

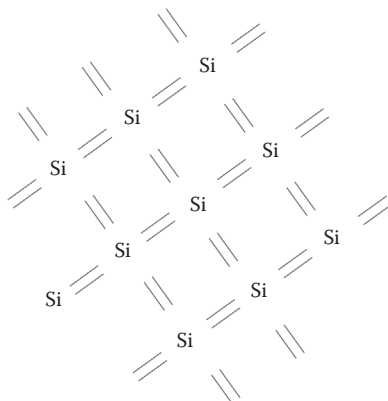


Figure 1.8 Two-dimensional representation of the silicon lattice.

When a number of silicon atoms are brought together, they form a diamond like silicon lattice; both the 3s level and the 3p level are broadened into bands that overlap and as the atoms approach their equilibrium position, these levels separate into two distinct bands with a gap between them. This band formation is illustrated in Figure 1.9, calculated for the case of nine such atoms. The nine allowed levels form quasi-continuous bands.

We refer to the lower band as the valence band and the upper band as the conduction band, and they are separated by the forbidden energy gap E_g as shown. This type of arrangement suggests that the silicon atom is already sharing its valence electrons throughout the lattice, a point we will make use of when describing conduction. Under certain conditions,

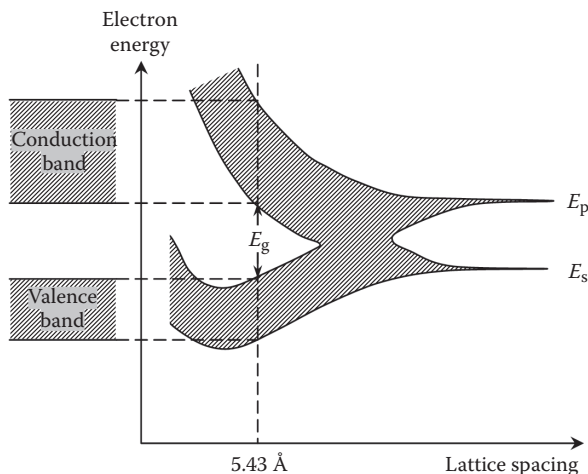


Figure 1.9 Formation of energy gap in a semiconductor as lattice atoms reach their equilibrium positions.

the valence electron can acquire sufficient energy to escape from this bond into the interstitial space becoming virtually free. It has now entered the conduction band, and the energy required to break the covalent bond is exactly equal to the bandgap energy of 1.1 eV in silicon. Thermal energy is an example of how this bond can be ruptured. Another example would be by photon absorption, where the energy of the incident photon is sufficient to break the bond. The excess energy is carried off by the subsequent photoelectron. By forming the energy gap, the quantum nature of every atom manifests itself throughout the semiconductor crystal and dominates its electrical characteristics.

The situation is, in fact, more complicated than described. We have described a *direct* bandgap. But in silicon (an indirect bandgap semiconductor), for the transition of an electron across the gap in either direction, momentum from a third source (usually lattice vibration, a ‘phonon’) is required (see Section 1.7.3). We see from the periodic table (Figure 1.7) that the crystalline Group 4 elements C (diamond), Si, and Ge are expected to be semiconductors. Figure 1.9 illustrates how the lattice spacing influences E_g . The closer the atomic packing, the larger the bandgap. The largest Group 4 bandgap, diamond (5.4 eV), has the closest atomic packing of all, resulting

in its extreme hardness. Because of the screening effect of the more tightly bound electrons, the energy gap decreases with atomic number Z . For germanium, it is 0.67 eV. It happens that the combining of atoms from either side of the Group 4 semiconductors into the so-called **3–5 (III–V)** compounds (marked orange in Figure 1.7) also produces semiconductors. They tend to be wide bandgap materials such as BN, AlN, GaAs, GaP, GaN, and InSb. Furthermore, **2–6 (II–VI)** compounds can also give important wide bandgap semiconductors (WBGSSs) such as CdTe. The lattice spacing (and hence, E_g and ω) can be influenced by both temperature and strain, and also the alloying of semiconductors, such as SiGe and CdZnTe. The latter is termed ‘bandgap engineering’ and will be further discussed in Chapter 10. The compounds involving elements closer to the edges of the periodic table (Figure 1.7) form weaker bonds by transferring electrons. They are thus more ionic in nature.

1.4 Fermi–Dirac Statistics

At very low temperatures, the free electrons in a metal fill the conduction band up to a characteristic energy called the Fermi energy, E_F . As the temperature rises, this abrupt falloff in the electron distribution, $n(E)$, is smoothed out according to the Fermi–Dirac distribution $F(E)$, which gives the probability that an electron quantum energy state is filled.

$$1/F(E) = \exp\{(E - E_F)/kT\} + 1 \quad (1.4)$$

This is illustrated in Figure 1.10, which shows the Fermi–Dirac distribution (a) (b) (c), for three increasing temperatures.

As the temperature increases, the tail of the Fermi–Dirac distribution can extend above zero energy (the ‘vacuum’ energy), and electrons can be evaporated off the surface (thermionic emission). Note that the Fermi–Dirac distribution value always remains half of its maximum value at the Fermi energy E_F . The concentration of electrons $n(E)$ is the product of the density of states available and the Fermi–Dirac

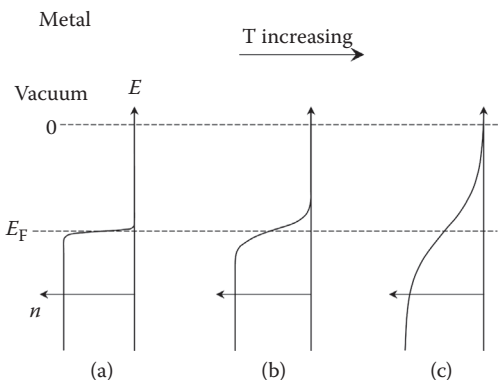


Figure 1.10 Fermi-Dirac distribution in metal. (a) Distribution at low temperature, (b) distribution at normal temperatures, and (c) distribution at high temperatures.

probability distribution of filling them. The diffusion of electrons will require that E_F remains constant throughout the metal if the metal has uniform properties.

At low temperatures and with no radiation of any sort present, semiconductors are, for all practical purposes, insulators and even at room temperature they never conduct as well as metals. When an electron makes the leap into the conduction band, two significant things happen. It upsets the charge neutrality of the site it came from (leaving an excess positive charge associated with the site), and it leaves an unoccupied electron state in the valence band as shown in Figure 1.11.

Thus, another electron from the valence band can take its place (itself creating a hole), and so effectively the ‘hole’ with its associated positive charge can move incrementally through the crystal. In an electric field, it moves in a way analogous to a positive carrier of charge and contributes to the conduction. This conduction is illustrated in Figure 1.12.

The holes and electrons are termed positive and negative ‘charge carriers’, and their densities in the semiconductor are represented by p and n . The motion of the charge carriers is characterised by their mobility μ in the semiconductor in terms of their drift velocity v in the presence of an electric field E . Thus,

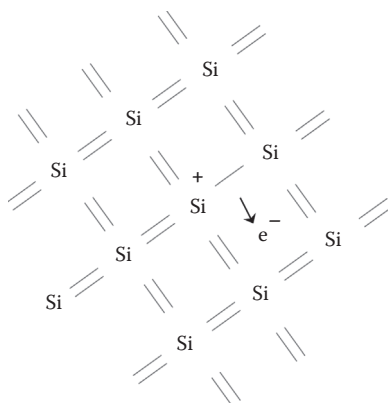


Figure 1.11 Electron moving into the conduction band.

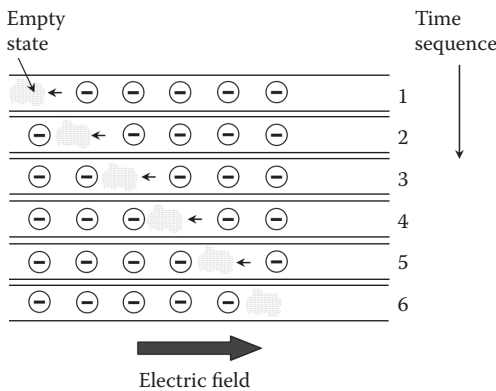


Figure 1.12 Movement of a hole in the presence of an electric field.

$$v = \mu E. \quad (1.5)$$

Because the mobility of carriers is dependent on scattering off the crystal lattice vibrations, termed ‘phonon scattering’ (and as we will see later, any impurities), it increases rapidly as the temperature is lowered. Figure 1.13 shows the variation of electron and hole mobility with temperature for silicon and germanium.

Unlike electrons, the holes cannot be regarded as point charges as they are associated with a distortion over many unit cells of the lattice and therefore not localised. As a result,

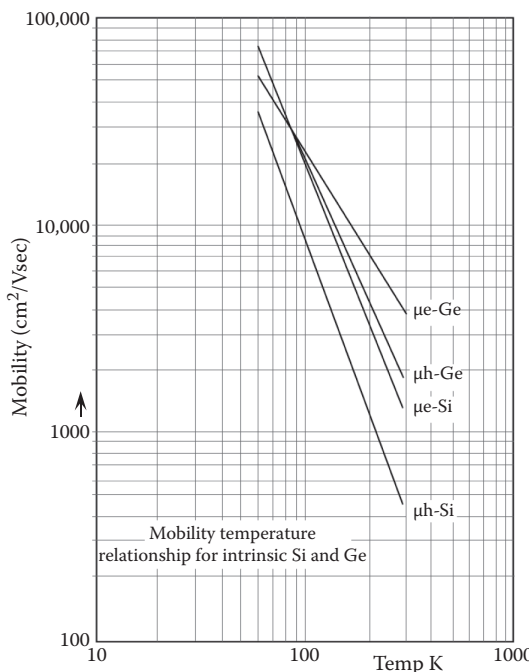


Figure 1.13 Mobility as a function of temperature.

their effective mass is higher and their mobility generally, lower and they are more prone to being trapped, for example, by dislocations or impurities in the lattice. As the field is increased, v increases linearly but reaches saturation velocity v_s when the energies become larger than the magnitude of the thermal energies. This occurs for electrons in silicon at room temperature at fields above ~ 10 kV/cm and at 100 K for silicon and germanium at fields above ~ 1 kV/cm, where $v_s \sim 10^7$ cm/s. The situation is not very different for holes. For cooled silicon and germanium detectors these fields are normally exceeded and we can assume near-saturation velocity for carriers. At fields another order of magnitude above (greater than ~ 100 kV/cm in silicon at room temperature), the electrons and holes can be accelerated sufficiently to cause ‘impact ionisation’. At very high fields, an avalanche of carriers can be produced effectively increasing the charge gain considerably. This effect is used in avalanche photodiodes (APDs), and we will

devote Section 7.2 to these photodiodes (used as x-ray detectors) later.

The mobility μ , involving the velocity of charges or—in other words—an electric current, can be related to electric resistance via Ohm's law

$$\Delta V = IR.$$

If we consider an element with area A through which the charge due to electrons moves dx in a time dt , Ohm's law gives

$$dV = (A\eta edx/dt)(\rho dx/A), \quad (1.6)$$

where ρ is the resistivity. In terms of the electric field, E , it follows from 1.5 that

$$E = -dV/dx = nev\rho.$$

Using Equation 1.5 for v ,

$$\rho = 1/(ne\mu).$$

Considering holes as well as electrons, this is usually written as the conductivity σ ($= 1/\rho$)

$$\sigma = e[n\mu(n) + p\mu(p)]. \quad (1.7)$$

Because it is always physically the movement of electrons, the mobility of the hole $\mu(p)$ in the valence band is of the same order of magnitude as the mobility of electrons $\mu(n)$ in the conduction band. Indeed, the mobility of holes can even, in some circumstances, exceed that of electrons as it does in GaAs and Ge (at LNT). The type of conduction described above is known as ‘intrinsic’ conduction, because it is an intrinsic property of the semiconductor alone. Intrinsic conduction can be produced by energetic vibrations in the crystal lattice (thermal ‘phonons’ or in other words, heat) or by ionising radiation. A detector based on the latter would be termed an ‘intrinsic detector’, and an example is the HPGe detector. Note that, in these circumstances, for every electron promoted to the conduction

band, there is a corresponding hole in the valence band. Thus, if n_i is the density of negative electrons and p_i is the density of positive holes in an *intrinsic* semiconductor then

$$n_i = p_i. \quad (1.8)$$

In this case, 1.7 reduces to

$$\sigma = en_i[\mu(n) + \mu(p)]. \quad (1.9)$$

The density of intrinsic carriers n_i is a strong function of temperature, as shown in Figure 1.14.

These intrinsic carriers are the ‘quiescent bubbles in our beer analogy detector’, and it illustrates why cooling (especially of germanium) is usually necessary. The Fermi–Dirac distribution for the valence band still applies for semiconductors but extends across the energy gap. The relevance of the Fermi energy E_F is now as a reference level at which the distribution falls to half maximum value, and so is the energy at

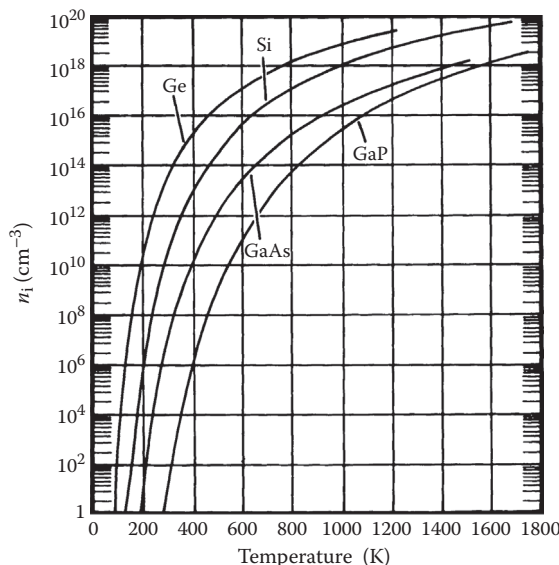


Figure 1.14 Carrier density as a function of temperature.

which the probability of finding an electron is equal to that of finding a hole. In intrinsic semiconductors, E_F is ‘pinned’ to mid-gap energy. As mentioned above, the concentration of electrons is the product of the density of available states and the Fermi–Dirac probability distribution. In an intrinsic semiconductor there are no such states in the energy gap. Figure 1.15 illustrates the band diagram for an intrinsic semiconductor at two different temperatures, (a) and (b). The mobile charges are depicted as the ‘wheels’ \oplus , \ominus (fixed charges are depicted as symbols + and -).

In case (b), the temperature is high enough for electrons to leap the energy gap, producing mobile electrons in the conduction band and mobile holes in the valence band. The electrons quickly relax back down to the lowest levels in the conduction band, and the holes relax back (holes being the absence of electrons ‘fall upward’) to the highest levels in the valence band.

In thermal equilibrium, the intrinsic carrier concentration n_i in the conduction band can be shown [4] to be given by

$$n_i^2 = N_C N_V \exp(-E_g/kT), \quad (1.10)$$

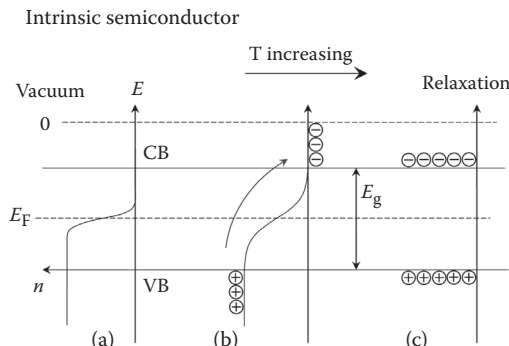


Figure 1.15 Intrinsic semiconductor bandgap and charge excitation. (a) At low temperatures the bands are free from charge, (b) as temperatures increase electrons cross the gap to populate many levels in the conduction band leaving holes in the valence band, and (c) as the excited electrons lose kinetic energy they relax back to the bottom of the conduction band and the holes move upwards to the top of the valence band.

where N_C and N_V are the effective density of states at the conduction and valence band edges, respectively. This leads to the relation

$$n_i = CT^{3/2} \exp(-E_g/2kT), \quad (1.11)$$

where C is a constant.

At normal temperatures, the exponential term dominates and the electrical conductivity increases rapidly with increasing temperature (unlike metals) and is reduced considerably in wide bandgap materials such as GaAs (see Figure 1.14).

1.5 Doping of Semiconductors

To make practical semiconductor devices (diodes, transistors, ICs), the electrical conductivity is increased by several orders of magnitude by adding to (or ‘doping’) the semiconductor with small amounts of specific impurity atoms. These dopant atoms occupy sites normally occupied by the semiconductor atom itself and have the effect of either *donating* an extra electron into the conduction band or forming a hole in the valence band. This hole can *accept* an electron from the conduction band. The two types of dopants are known as *donors* and *acceptors*. Respective examples are phosphorus (P) and boron (B). This is illustrated in Figure 1.16.

The Coulomb force binding this electron to the P atom is reduced by the screening effect of other electrons, by the dielectric constant (~12 for silicon), and its effective orbit radius is increased by the same factor. This results in a lowering of the bond energy by a factor of 144 from 1.1 eV to a value of ~7.6 meV. The P atom can be regarded as a large ‘hydrogen-like’ atom extending over a great many lattice sites. The donor P atom is at first electrically neutral, but the electron being weakly bound will move away from the site under the influence of an electric field and/or thermal energy. This then exposes the fixed positive charge on the P nucleus (the donor site) that will act to terminate electric field lines and scatter carriers as they move through the crystal. This adds to the

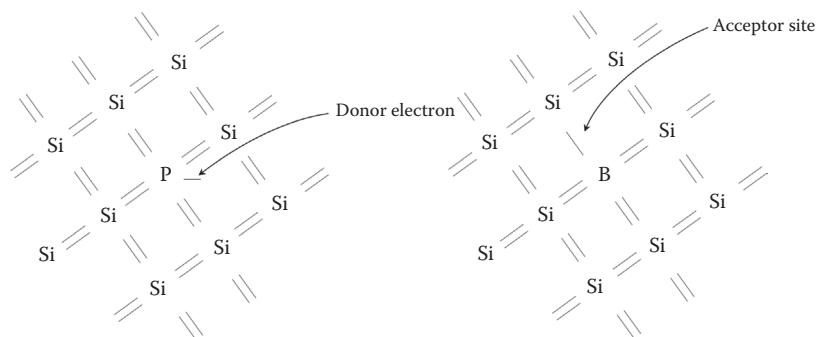


Figure 1.16 Illustrating a donor atom ‘P’ (resulting in a mobile electron) and an acceptor atom ‘B’ (resulting in a mobile hole) in the Si lattice.

thermal scattering of carriers discussed above and decreases their mobility considerably.

Likewise, the B atom in Figure 1.16 can lose its associated hole when an electron fills it (or ‘combines’ with it), charging it negatively and making it also a scattering site (the B acceptor site). The Si atom that supplied the electron to the acceptor site becomes positively charged, and in this way the hole is associated with a positive charge that moves with it through the crystal as described in Section 1.4. Because the conduction is now dominated by externally introduced impurities, the type of conduction caused by the motion of these mobile holes and electrons is termed ‘extrinsic’ conduction. The conduction in conjugate polymers is quite different and is attributable to the alternating double and single covalent bonds within the structure.

In the above example of doped semiconductors, the majority of charge carriers are negative in the donor case and positive in the acceptor case and they are referred to as n-type and p-type semiconductors. The carriers are referred to as the *majority carriers* (electrons in n-type and holes in p-type) and the intrinsic thermal carriers, or carriers generated by radiation, supply the *minority carriers*. If we dope the semiconductor with a density of N_D donors, we get an extra density of majority carriers $n = N_D$ (free electrons) without introducing any holes at all. Likewise, in a p-type semiconductor, we get an extra $p = N_A$. Normally, the densities of carriers introduced by doping far exceeds the density

of intrinsic carriers, and we can equate $p \sim N_A$ and $n \sim N_D$. It is important to realise that the crystal in all these cases remains overall electrically neutral. This is known as the principle of neutrality. In terms of the band diagrams, the acceptor impurities give rise to energy levels within the band-gap close to the valence band and the donor impurities give rise to energy levels close to the conduction band. This has the effect of displacing the Fermi level E_F downward from mid-gap position in the first case (p-type semiconductor) and upward in the second (n-type semiconductor). This is illustrated in Figure 1.17.

Such ‘band diagrams’ must always be interpreted as showing the potential energy of *electrons*. The majority carriers introduced by these impurities dominate the conductivity of a ‘doped’ semiconductor. This dominates over the effect of any decrease in mobility caused by them, and Equation 1.7 becomes

$$\sigma = e[N_D\mu(n) + N_A\mu(p)].$$

Figure 1.18 shows the effect of doping on the resistivity of silicon at room temperature.

Because μ for holes is $\sim 1/3$ that for electrons, p-type materials have $\sim 3\times$ the resistivity of n-type for the same level of doping. Of course, a semiconductor can be doped with both donors and acceptors. Whether the material is n-type or p-type will depend on the sign of $(N_D - N_A)$. When the level of both types of dopants is very high [i.e., when $(n \sim p)$], the Fermi level is ‘pinned’ to near mid-gap. This situation is sometimes (somewhat misleadingly) termed ‘intrinsic’.

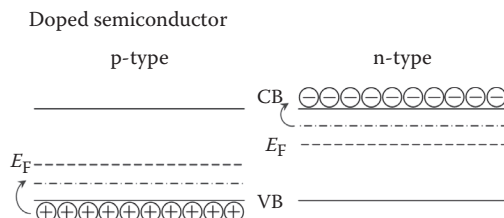


Figure 1.17 Movement of the Fermi level in a doped semiconductor.

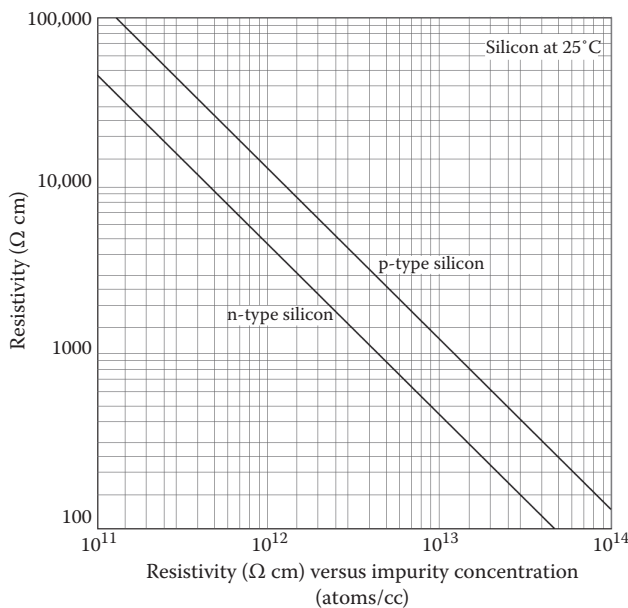


Figure 1.18 Resistivity vs. doping concentration at 25°C.

1.5.1 Law of Mass Action

Doping takes the carrier densities from n_i to n and $p_i (=n_i)$ to p . As we have seen, the holes and electrons can recombine and the rate at which this happens will be proportional to the product of their densities np . At a given temperature, the thermal generation rate of holes and electrons in the doped semiconductor will only depend on the density of the valence bonds in the crystal, and this is always far higher than the density of impurity atoms. The generation rate will therefore be virtually the same as for the undoped intrinsic material, and the recombination rate for this, by Equation 1.8, is

$$n_i p_i = n_i^2.$$

However, by the law of mass action in thermal equilibrium, the recombination rate must be equal to the generation rate (in both intrinsic and extrinsic material) and we must have

$$np = n_i^2. \quad (1.12)$$

This equation describes the equilibrium between recombination and generation. Thus, the effect of adding mobile electrons by adding donor impurities has the effect of *decreasing* the hole concentration p . Similarly for acceptor impurities, the electron concentration n is suppressed. For example, in n-type silicon at room temperature, with modest donor impurity concentration (say one atom in 4×10^{10}), its conductivity is dominated by electrons. The generation rate n_i^2 depends on the density of states at the bottom of the conduction band, the temperature T , and energy gap E_g of the semiconductor as shown by Equation 1.10. Because it does not depend on the Fermi level, it applies to doped as well as intrinsic semiconductors.

If charge generation dominates, we have nonequilibrium conditions, and

$$np \ll n_i^2.$$

This is the case, for example, where we have a field (as in the depletion layer of a biased p–n junction diode) that separates the holes and electrons before they can recombine. However, we have a ‘quasi-equilibrium’ condition where

$$np \sim \text{constant}. \quad (1.13)$$

If the temperature is low enough, we might expect $p = 0$ for n-type material, but this is not true. There is always a hole density given by Equation 1.12

$$p = n_i^2/n = n_i^2/N_D.$$

Another case of nonequilibrium is the injection of charge into the base region in transistor action. We might expect that the density of minority carriers could exceed the density of majority carriers! However, this is also not so as the system will always adjust toward charge neutrality. A corresponding

opposite charge is drawn from the base contact in a very short time (dielectric relaxation time, $\tau = \epsilon\epsilon_0\rho$). Thus, the density of minority carriers never exceeds the density of majority carriers.

1.5.2 Depletion Layers and Band Bending

Consider an n-type semiconductor (right-hand side of Figure 1.19). The left-hand side is an isolated uniform material, which is occupied by electrons, but we will not specify the material just yet. It could, for example, be a metal, another crystalline semiconductor, or some amorphous material. The situation where they are not in contact is shown in Figure 1.19a. We will bring these two materials into intimate contact in what we will call a ‘junction’. Assume that both have populations of electrons described by Fermi levels E_F in each. Their difference is shown as $\Delta\phi$, but in isolation they do not have any bearing on each other.

If they are first connected together by a conducting wire, because of the difference in Fermi levels and the need to

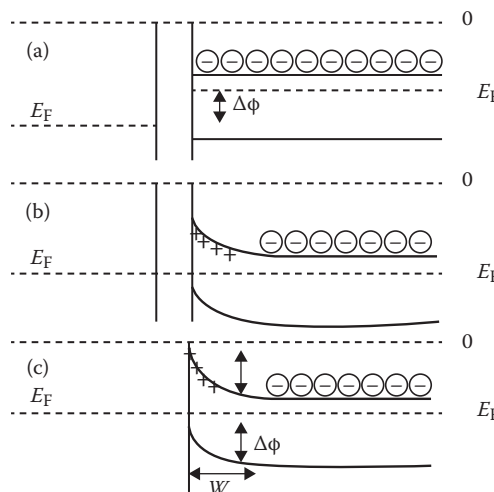


Figure 1.19 Illustration of how, in equilibrium, bands have to bend to allow the Fermi level to be continuous throughout the structure. (a) Unspecified material on the left hand side not in contact with the n-type semiconductor on the right hand side, (b) material now connected to the semiconductor with a wire, and (c) material in intimate contact with the semiconductor.